Electronic Supplementary Material (ESI) for New Journal of Chemistry.

An IMPLCATION-logic based fluorescent probe for sequential detection of Cu^{2+} and phosphates in living cells

Meixiang Wang, Xiaoxiao Niu, Rui Cao, Mengyu Zhang, Huajie Xu*, Fuying Hao and Zhaodi Liu*

School of Chemistry and Materials Engineering, Fuyang Normal University, Fuyang, Anhui 236037, P. R. China. E-mail: zhaodi_liu@163.com, 2000xhj@163.com

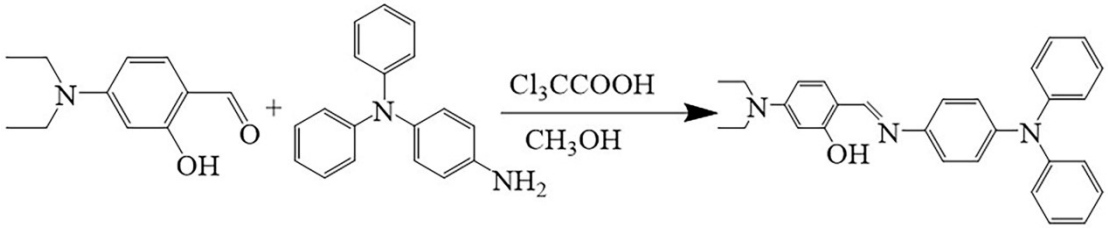

Scheme S1 The synthesis of HL

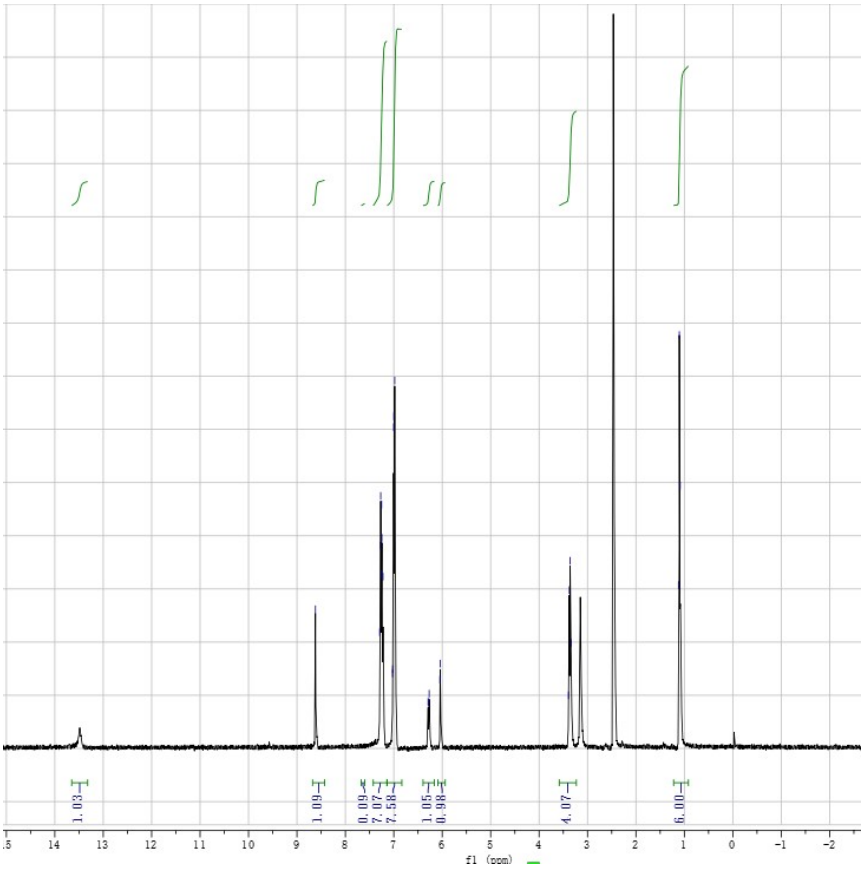

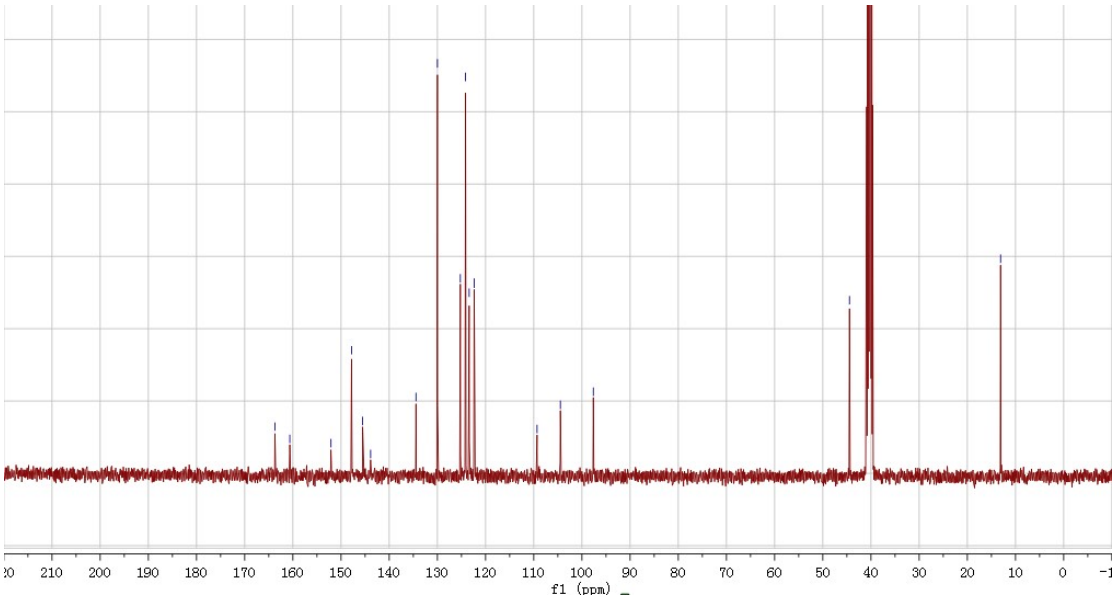

Fig.S1. ^{1}H NMR (upper) spectra and ^{13}C NMR (bottom) spectra of **HL** in d_6-acetone.

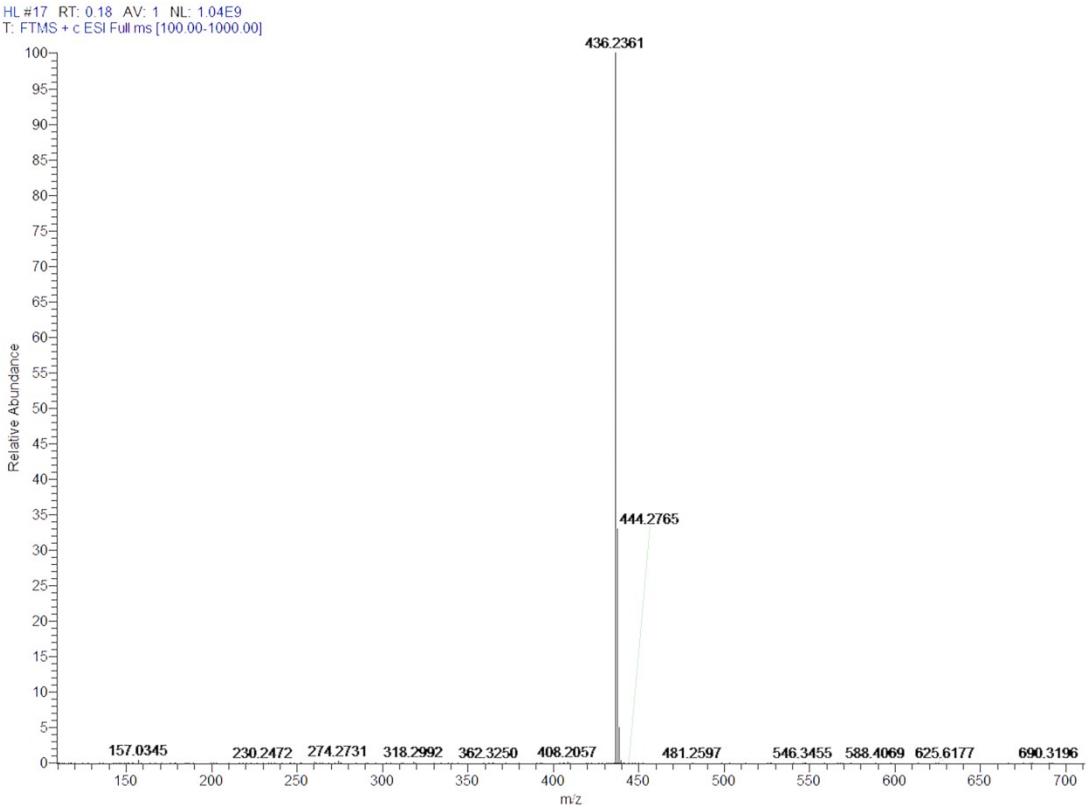

Fig.S2.ESI-MS spectrum of HL.

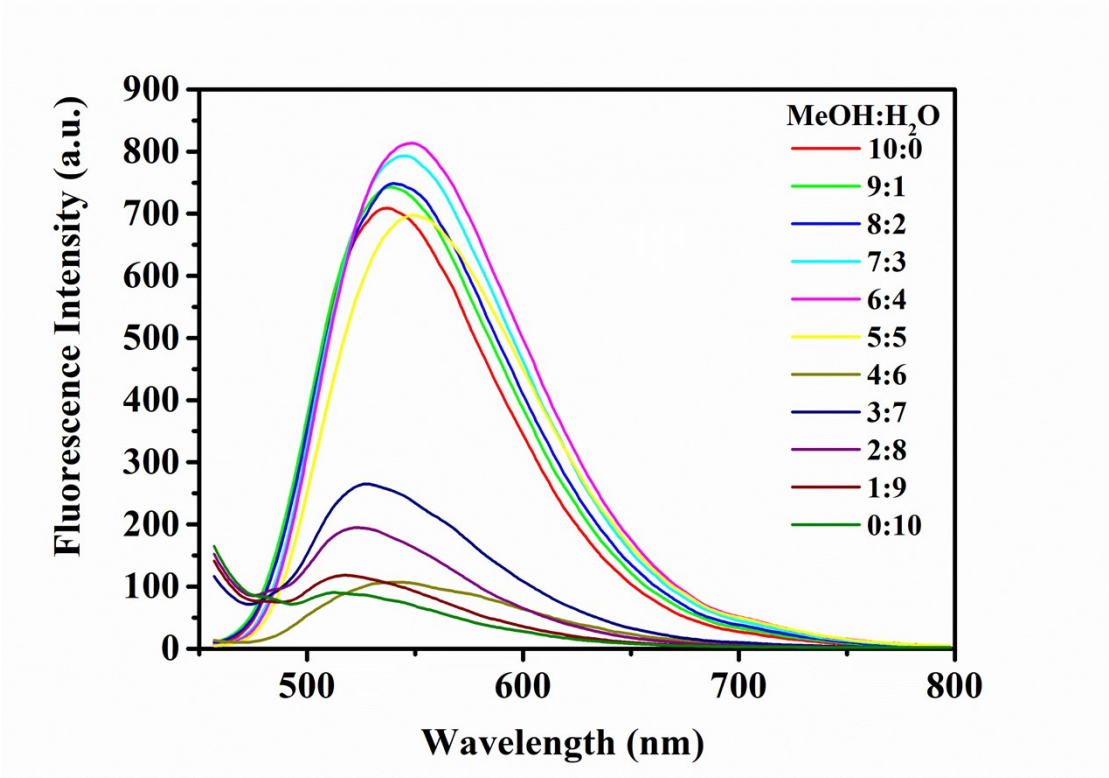

Fig.S3. HL fluorescence diagram at different moisture contents

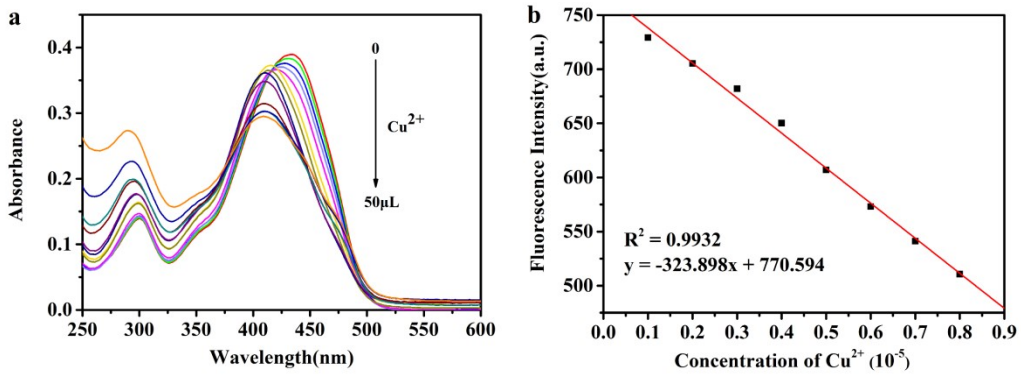

Fig.S4. (a) The absorbance titration of probe HL (10 μM) with Cu^{2+} (16.7 μM); (b) Fluorescence spectroscopy HL on Cu^{2+} titration working curve(in methanol/HEPES ($V_{methanol}/V_{HEPES}$ = 7/3)) (λ_{ex} = 450 nm)

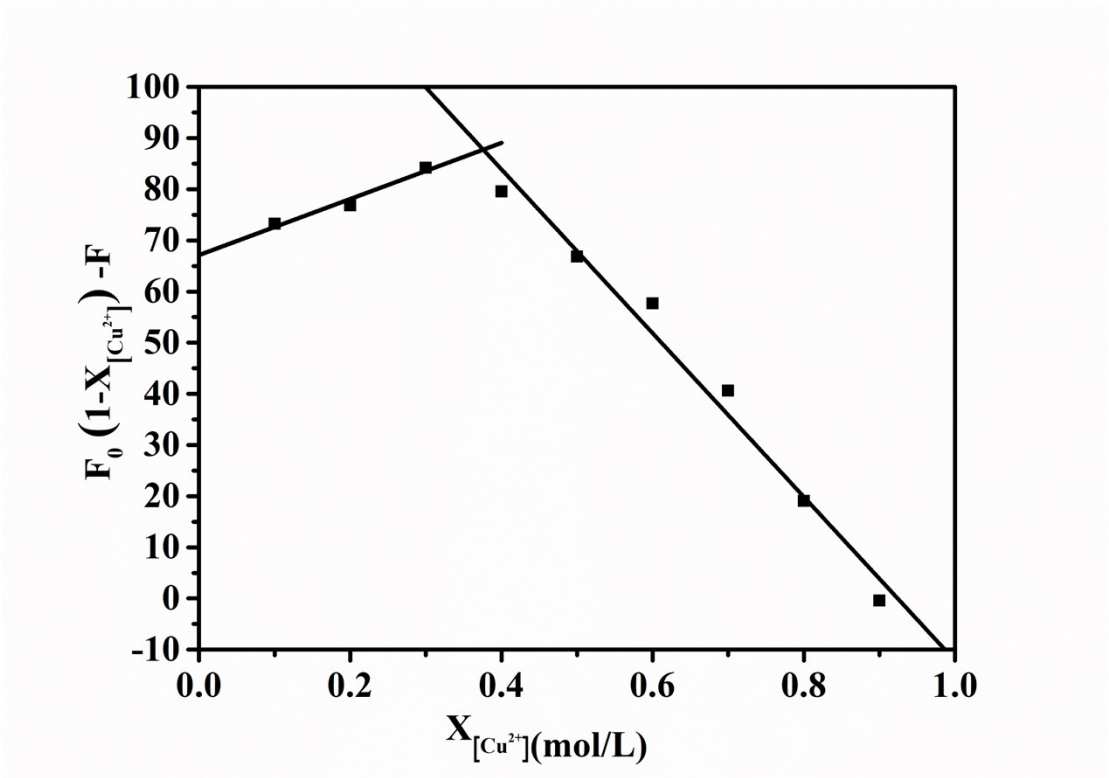

Fig.S5. Job plot determining the binding mode of L-Cu in methanol/HEPES ($V_{methanol}/V_{HEPES}$ = 7/3)

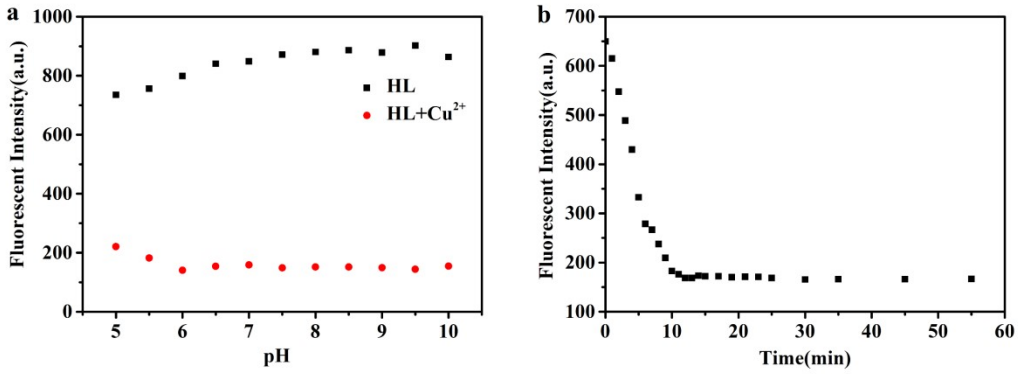

Fig.S6. (a)The effect of pH on probe **HL** with or without Cu^{2+};(b) The time-dependent on probe **HL** with Cu^{2+} (λ_{em} = 550 nm).

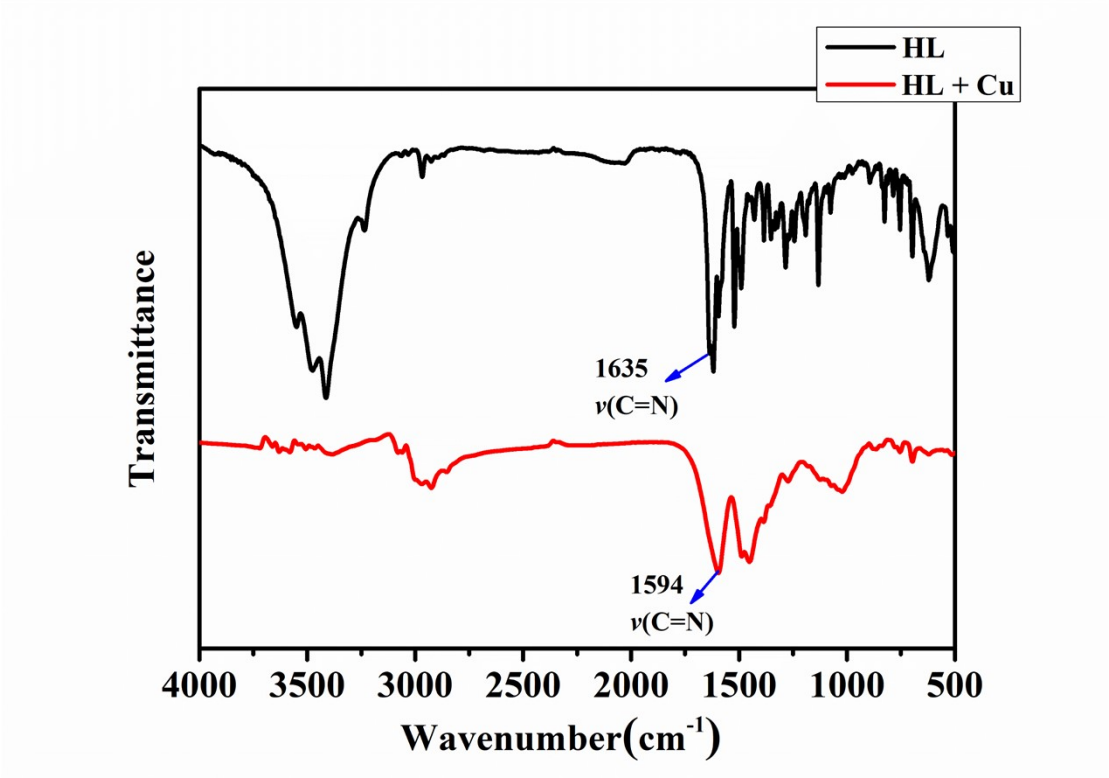

Fig.S7. The IR spectra of HL (black) and L-Cu^{2+} complex(red)

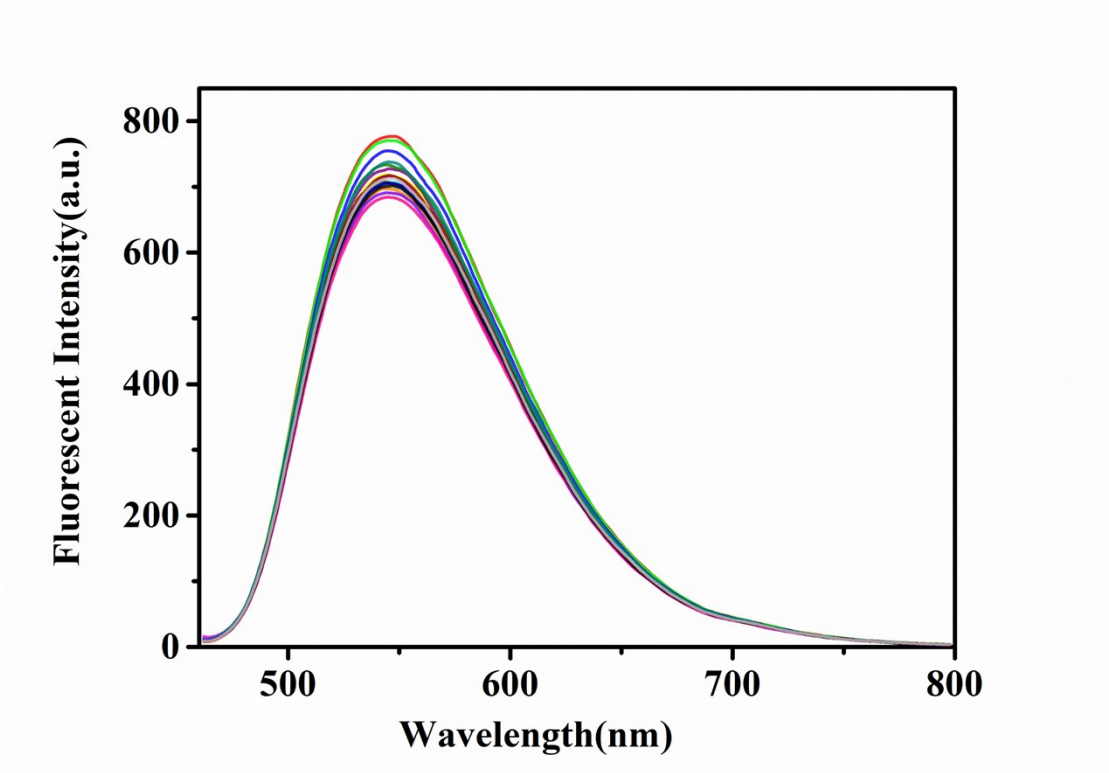

Fig.S8. The fluorescence spectrogram of HL with anions （F^-, Cl^-, Br^-, I^-, Ac^-, NO_3^-, ClO^-, HCO_3^-, HSO_3^-, CO_3^{2-}, SO_3^{2-}, SiO_3^{2-}, SO_4^{2-}, $H_2PO_4^-$, HPO_4^{2-}, PO_4^{3-}, PPi^{4-}）(10

μM) (λ_{ex} = 450 nm)

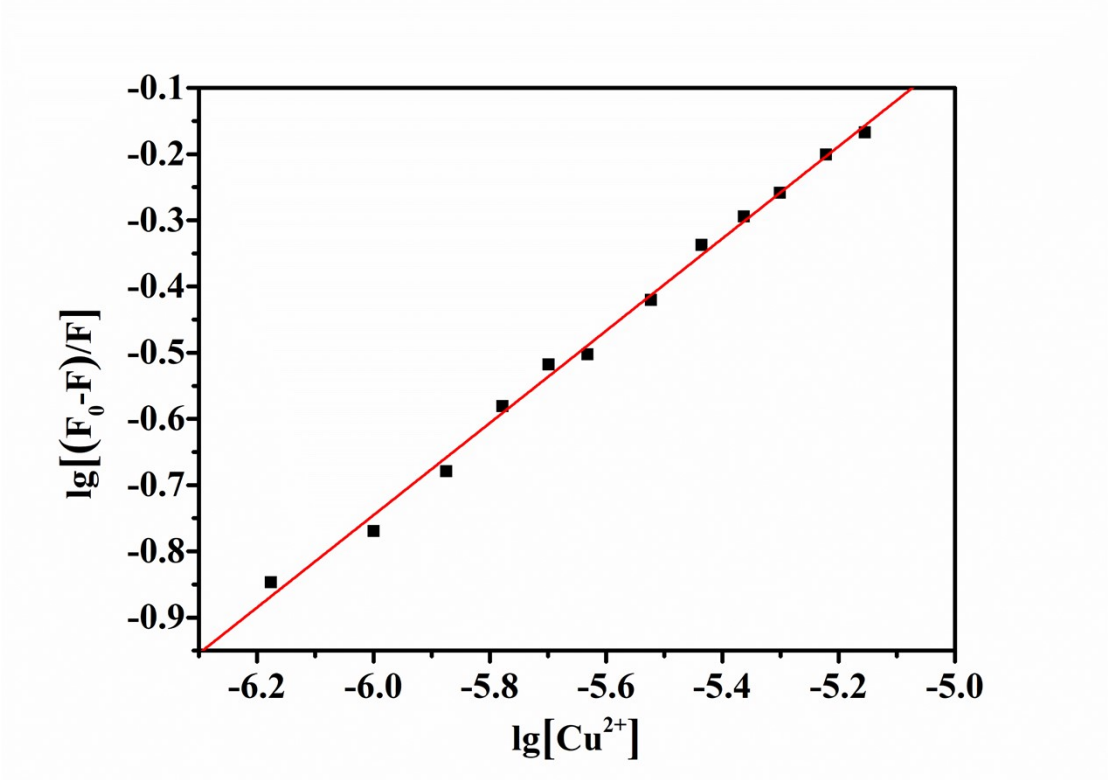

Fig.S9. Fitting of fluorescence titration of HL with Cu^{2+} in methanol/HEPES (pH = 7.00, 7/3, v/v). (λ_{ex} = 450 nm). The binding constant of HL and Cu^{2+} is 7.9×10^{-4} M^{-2}.

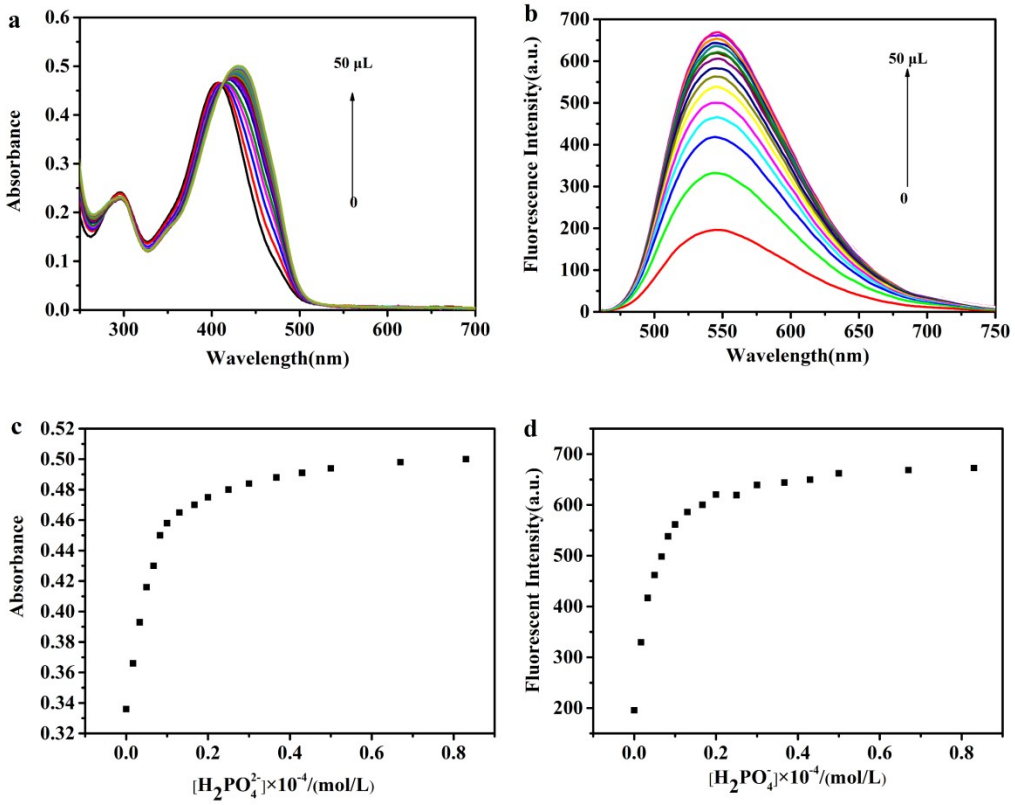

Fig.S10. The absorbance titration (a) and the fluorescence titration (b) of probe L-Cu (10 μM) with $H_2PO_4^-$ (16.7 μM) (λ_{ex} = 450 nm);(c) changes in absorbance at 450 nm against concentration of $H_2PO_4^-$ (in methanol/HEPES ($V_{methanol}/V_{HEPES}$ = 7/3)) (d) changes in fluorescence intensity at 450 nm against concentration of $H_2PO_4^-$ (in methanol/HEPES ($V_{methanol}/V_{HEPES}$ = 7/3)).

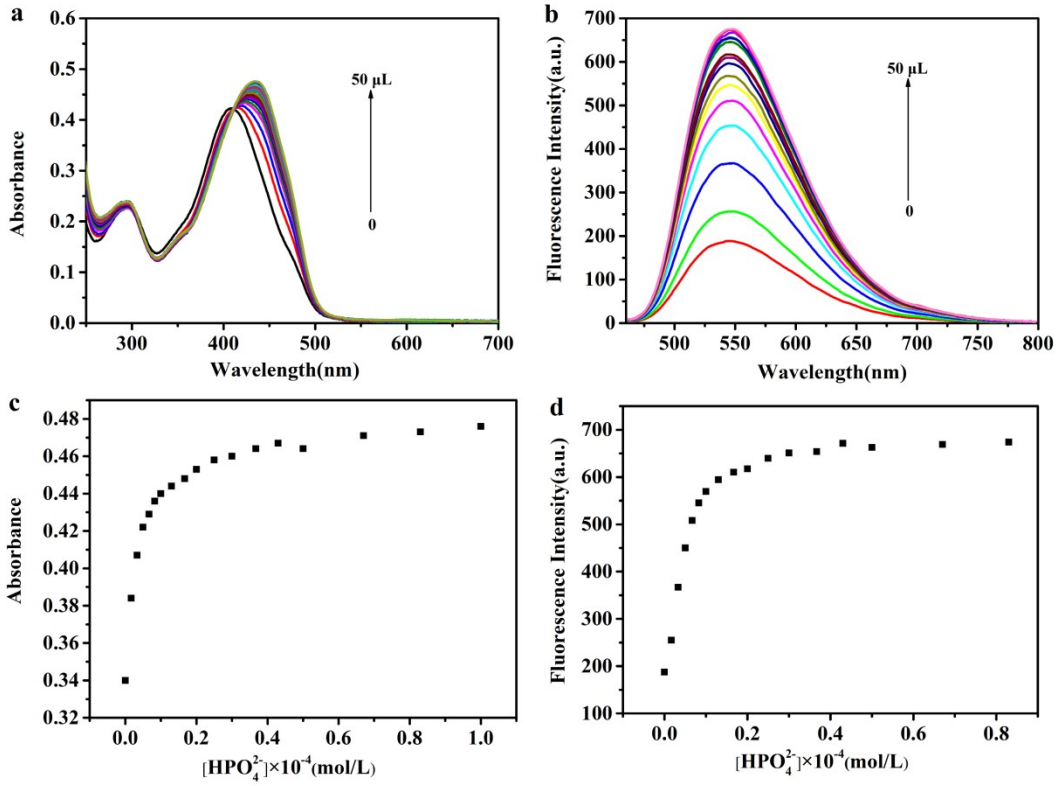

Fig.S11. The absorbance titration (a) and the fluorescence titration (b) of probe L-Cu (10 μM) with HPO_4^{2-} (16.7 μM) (λ_{ex} = 450 nm); (c) changes in absorbance at 450 nm against concentration of HPO_4^{2-} (in methanol/HEPES ($V_{methanol}/V_{HEPES}$ = 7/3)) (d) changes in fluorescence intensity at 450 nm against concentration of HPO_4^{2-} (in methanol/HEPES ($V_{methanol}/V_{HEPES}$ = 7/3)).

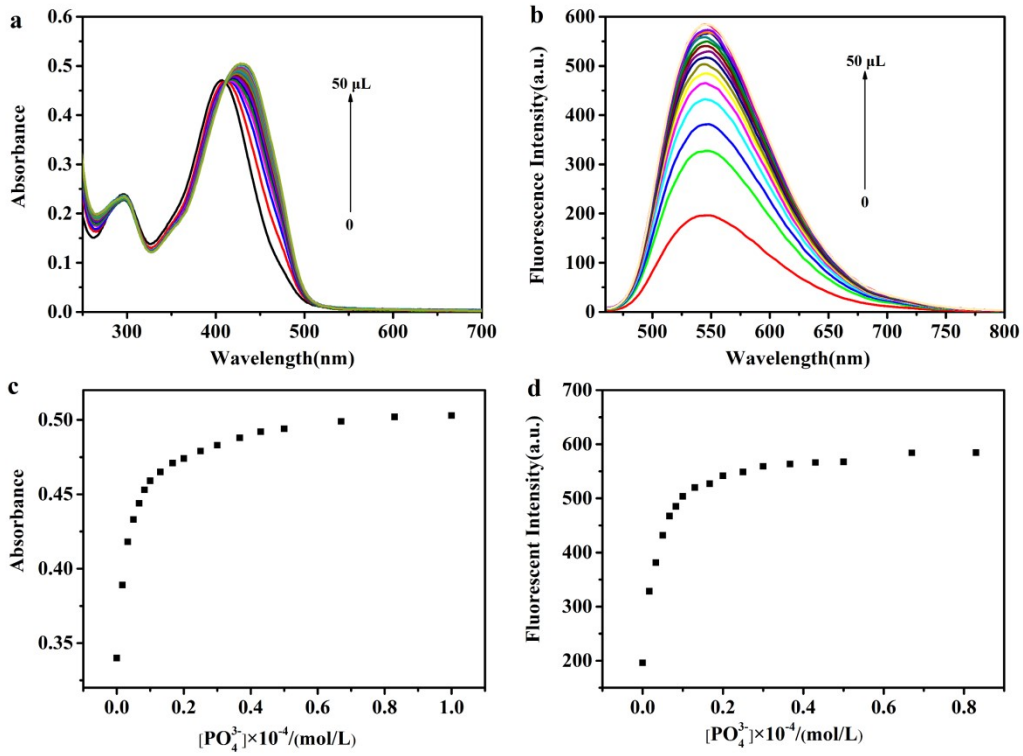

Fig.S12. The absorbance titration (a) and the fluorescence titration (b) of probe L-Cu (10 μM) with PO_4^{3-} (16.7 μM) (λ_{ex} = 450 nm);(c) changes in absorbance at 450 nm against concentration of PO_4^{3-} (in methanol/HEPES ($V_{methanol}/V_{HEPES}$ = 7/3)) (d) changes in fluorescence intensity at 450 nm against concentration of PO_4^{3-} (in methanol/HEPES ($V_{methanol}/V_{HEPES}$ = 7/3)).

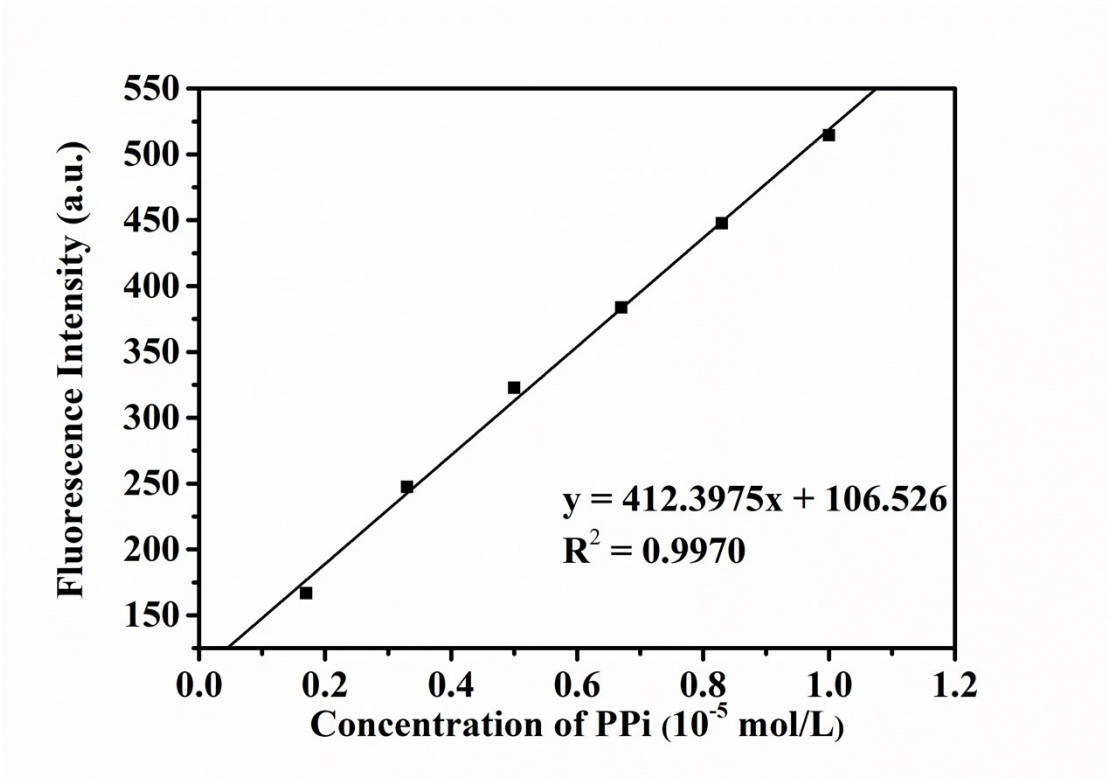

Fig.S13. The curve of Fluorescence Intensity with PPi concentration (0 – 16.7 μM).

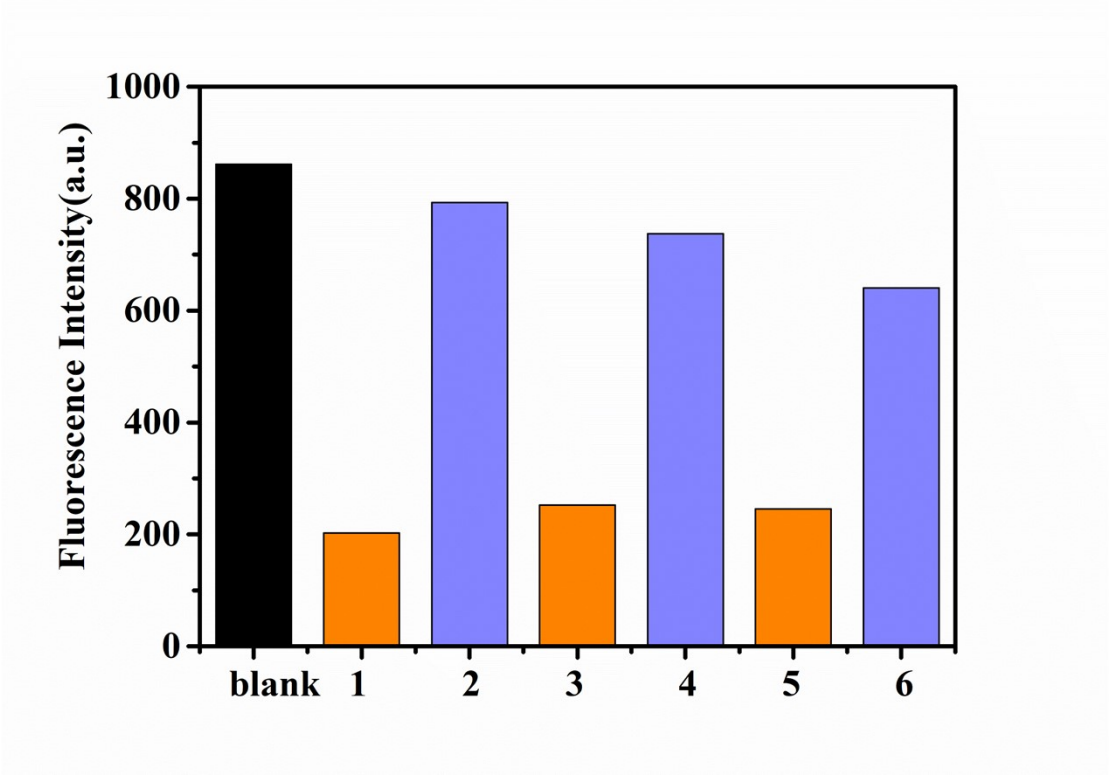

Fig.S14. Fluorescence peak intensity plots of HL with alternate addition of Cu^{2+} and PPi（1, 3 and 5 indicate addition of 30, 60 and 90 μLCu^{2+} ,respectively; 2, 4 and 6

indicate addition of 30, 60 and 90 μLPPi^{4-} ,respectively .）

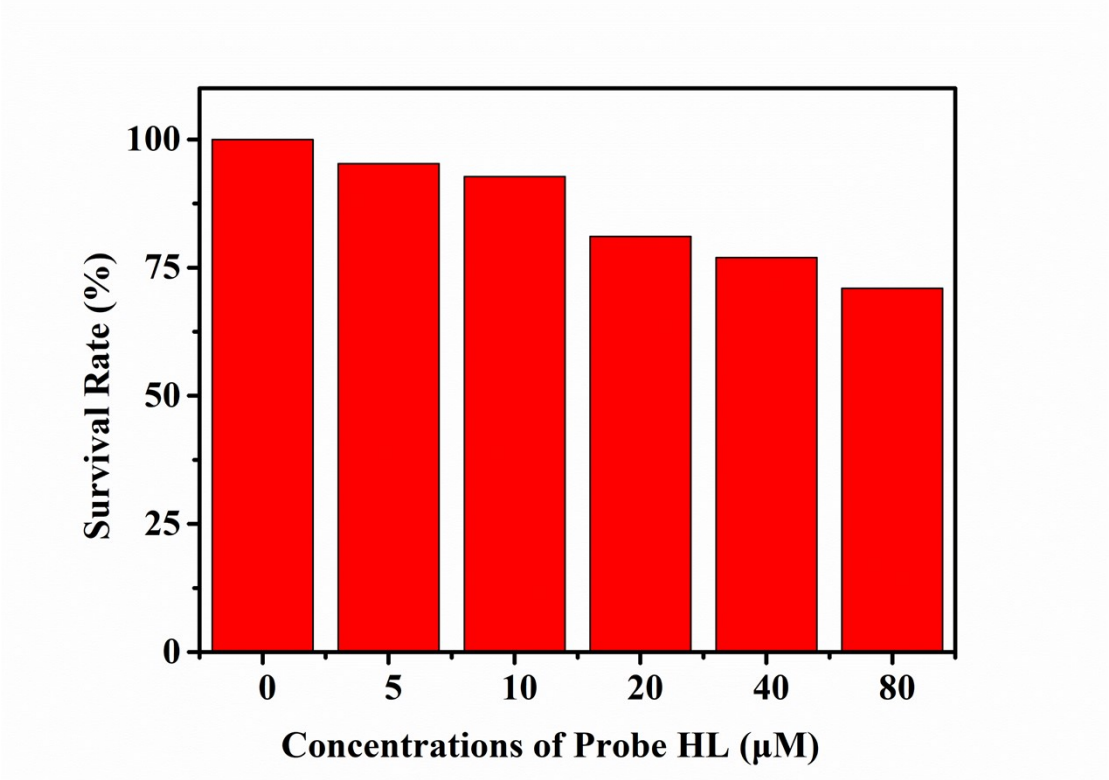

Fig.S15. Cytotoxicity experiments of Hela cells at various concentrations.